



**HAL**  
open science

## Differentiation of liver progenitor cell line to functional organotypic cultures in 3D nanofibrillar cellulose and hyaluronan-gelatin hydrogels.

Melina M Malinen, Liisa K Kanninen, Anne Corlu, Helena M Isoniemi,  
Yan-Ru Lou, Marjo L Yliperttula, Arto O Urtti

► **To cite this version:**

Melina M Malinen, Liisa K Kanninen, Anne Corlu, Helena M Isoniemi, Yan-Ru Lou, et al.. Differentiation of liver progenitor cell line to functional organotypic cultures in 3D nanofibrillar cellulose and hyaluronan-gelatin hydrogels.. *Biomaterials*, 2014, 35 (19), pp.5110-5121. 10.1016/j.biomaterials.2014.03.020 . hal-01134773

**HAL Id: hal-01134773**

**<https://univ-rennes.hal.science/hal-01134773>**

Submitted on 29 Mar 2016

**HAL** is a multi-disciplinary open access archive for the deposit and dissemination of scientific research documents, whether they are published or not. The documents may come from teaching and research institutions in France or abroad, or from public or private research centers.

L'archive ouverte pluridisciplinaire **HAL**, est destinée au dépôt et à la diffusion de documents scientifiques de niveau recherche, publiés ou non, émanant des établissements d'enseignement et de recherche français ou étrangers, des laboratoires publics ou privés.



# Differentiation of liver progenitor cell line to functional organotypic cultures in 3D nanofibrillar cellulose and hyaluronan-gelatin hydrogels



Melina M. Malinen<sup>a</sup>, Liisa K. Kanninen<sup>a</sup>, Anne Corlu<sup>b</sup>, Helena M. Isoniemi<sup>c</sup>, Yan-Ru Lou<sup>a</sup>, Marjo L. Yliperttula<sup>a</sup>, Arto O. Urtti<sup>a,d,\*</sup>

<sup>a</sup>Centre for Drug Research, Division of Pharmaceutical Biosciences, Faculty of Pharmacy, University of Helsinki, P.O. Box 56, FI-00014 Helsinki, Finland

<sup>b</sup>Inserm UMR991, Liver Metabolism and Cancer, Université de Rennes 1, F-35043 Rennes, France

<sup>c</sup>HUS, Transplantation and Liver Surgery Clinic, P.O. Box 340, FI-00029 HUS, Finland

<sup>d</sup>School of Pharmacy, University of Eastern Finland, P.O. Box 1627, FI-70211 Kuopio, Finland

## ARTICLE INFO

### Article history:

Received 8 January 2014

Accepted 11 March 2014

Available online 1 April 2014

### Keywords:

3D Cell culture

Hepatocyte

Multicellular spheroids

Cell differentiation

Nanocellulose

Organotypic

## ABSTRACT

Physiologically relevant hepatic cell culture models must be based on three-dimensional (3D) culture of human cells. However, liver cells are generally cultured in two-dimensional (2D) format that deviates from the normal *in vivo* morphology. We generated 3D culture environment for HepaRG liver progenitor cells using wood-derived nanofibrillar cellulose (NFC) and hyaluronan-gelatin (HG) hydrogels. Culture of undifferentiated HepaRG cells in NFC and HG hydrogels induced formation of 3D multicellular spheroids with apicobasal polarity and functional bile canaliculi-like structures, structural hallmarks of the liver tissue. Furthermore, hepatobiliary drug transporters, MRP2 and MDR1, were localized on the canalicular membranes of the spheroids and vectorial transport of fluorescent probes towards the biliary compartment was demonstrated. Cell culture in 3D hydrogel supported the mRNA expression of hepatocyte markers (albumin and CYP3A4), and metabolic activity of CYP3A4 in the HepaRG cell cultures. On the contrary, the 3D hydrogel cultures with pre-differentiated HepaRG cells showed decreasing expression of albumin and CYP3A4 transcripts as well as CYP3A4 activity. It is concluded that NFC and HG hydrogels expedite the hepatic differentiation of HepaRG liver progenitor cells better than the standard 2D culture environment. This was shown as improved cell morphology, expression and localization of hepatic markers, metabolic activity and vectorial transport. The NFC and HG hydrogels are promising materials for hepatic cell culture and tissue engineering.

© 2014 The Authors. Published by Elsevier Ltd. This is an open access article under the CC BY license (<http://creativecommons.org/licenses/by/3.0/>).

**Abbreviations:** 2D, two-dimensional; 3D, three-dimensional; ABC transporter, ATP-binding cassette transporter; ALB, Albumin; Calcein-AM, calcein-acetoxymethyl ester; CycloG, cyclophilin G (peptidylprolyl isomerase G); CYP, cytochrome P450; DMSO, dimethyl sulfoxide; dPBS, Dulbecco's modified phosphate salt buffer; ECM, extracellular matrix; F-actin, filamentous actin; HBSS, Hank's balanced salt solution; HG, hyaluronan-gelatin hydrogel (Extracel™); HNF4A, hepatic nuclear factor 4A; MDR1, multidrug resistance protein 1 (ABCB1, P-glycoprotein); MRP, multidrug resistance-associated protein; MRP2, ATP-binding cassette sub-family C member 2 (ABCC2); NFC, nanofibrillar cellulose (Growdex™); PBS, phosphate salt buffer; RT, room temperature; RT-PCR, real time polymerase chain reaction.

\* Corresponding author. Centre for Drug Research, Division of Pharmaceutical Biosciences, Faculty of Pharmacy, University of Helsinki, P.O. Box 56, FI-00014 Helsinki, Finland. Tel.: +358 919159636; fax: +358 919159725.

E-mail address: [arto.urtti@helsinki.fi](mailto:arto.urtti@helsinki.fi) (A.O. Urtti).

## 1. Introduction

Pharmaceutical industry, regulatory authorities, and academic investigators need liver cell cultures to predict and estimate metabolism, excretion and toxicity of drugs and other chemicals in the human liver. Due to the inter-species differences animals and animal cells lead frequently to misleading, and sometimes hazardous, estimates of pharmacokinetics and toxicity in humans. Therefore, Food and Drug Administration of the United States has emphasized the need for improved preclinical cell models for drug development in their Critical Path Initiative.

Human liver microsomes are used to study xenobiotic metabolism, but the microsomes do not have drug transporters or transcription machinery. This limits seriously their usefulness in pharmacokinetics and toxicology. Primary human hepatocyte cultures in 2D are the gold standard in *in vitro* evaluation of hepatic

**Table 1**  
HepaRG cultures were performed in distinct culture dishes depending on the end-point analysis.

	Standard tissue culture treated 96-well plates	Ultra low Attachment 96-well plates (Corning Inc.)	Lab-tek chambered#1.0 borosilicate coverglass system (Thermo Scientific)	Lab-tek chamber slide system with Permanox® plastic (Thermo Scientific)	μ-plate 96-well plates (ibidi GmbH)
alamarBlue	2D	3D			
CYP activity	2D	3D			
PCR	2D	3D			
gDNA	2D	3D			
Live/dead			2D & 3D		
Transporter activity			2D & 3D		2D & 3D
Immuno-histochemistry				2D & 3D	

metabolism and toxicity. However, the availability of human primary hepatocytes is limited, they show substantial functional variability and restricted lifespan, and their drug transporter activity is low unless they are ‘sandwich-cultured’ [1,2]. Immortal human liver cell lines, such as HepG2 and HepaRG are widely used in *in vitro* studies [3,4]. Compared to HepG2 cells, HepaRG liver progenitor cells generate improved hepatic phenotype in culture and this continuous cell line has been successfully applied in the evaluation of chemicals and drug candidates [4–8]. However, 2D format of the current HepaRG cultures clearly deviates from the vectorial 3D morphology of the hepatocytes in the liver. Overall, the existing liver cell models are not satisfactory and more representative cell models are needed for biological research and drug and chemical testing.

Cellular phenotype can be tuned with the culture environment, particularly with extracellular matrix mimicking biomaterials. Preferably the biomaterials should provide fibrillar structures, extracellular matrix mimicking stiffness and hydrous environment with unrestricted permeation of nutrients and endogenous factors [9–13]. We investigated hydrogels of native wood-derived nanofibrillar cellulose (NFC) and hyaluronan-gelatin (HG) as supporting materials in the 3D culture of HepaRG liver progenitor cells.

## 2. Materials and methods

### 2.1. Biomaterials

Growdex™ nanofibrillar cellulose (NFC) hydrogel was obtained from UPM Corporation, Finland. The preparation and properties of NFC hydrogel have been described in detail earlier [12]. The NFC concentration of the hydrogel was 1.7 wt% and the product was sterile. Due to the used raw material, the NFC hydrogel contains also substantial amounts of hemicellulose, mainly xylene (25%), which generates a slightly anionic surface charge (−2 mV) on the fibrils. Extracel® (HG) hydrogel is based on thiol-modified hyaluronan, thiol-modified gelatin and crosslinker (polyethylene glycol diacrylate) (PEGDA) [21,22]. This material was obtained from Glycosan Biosystems, USA.

### 2.2. Human liver tissue

Human liver tissue was obtained from harvested organs for liver transplantation in the Transplantation and Liver Surgery Clinic (Helsinki, Finland). Donor livers were from brain dead male (age 41) and female (ages of 58, 13 and five) subjects with beating heart, normal liver function, negative hepatitis serology, and non-pathologic liver histology. The livers were flushed *in situ* with University of Wisconsin solution and kept at +4 °C until resection. Liver segments that were redundant for liver transplantations were sliced and stored at −70 °C in TRI reagent (Sigma–Aldrich) or at −20 °C in RNAlater (Qiagen). RNA was extracted (see paragraph for real time polymerase chain reaction). The research was authorized by National Supervisory Authority for Welfare and Health and by the Hospital District of Helsinki and Uusimaa Ethics Committee Department of Surgery.

### 2.3. HepaRG cell line

HepaRG cells have been derived from a liver tumor of a female patient who suffered from hepatitis C virus and hepatocarcinoma [23]. HepaRG cells are capable of differentiating into biliary-like epithelial cells (cholangiocyte-like cells) and hepatocyte-like cells. At low culture density, the cells express markers of early liver progenitors, and at confluence the cells will be committed to hepatocyte-like

differentiation [24]. The differentiation into mature hepatocyte-like cells is potentialized by dimethyl sulfoxide (DMSO) treatment. Subcultivation at low-density induces dedifferentiation of differentiated cells into early liver progenitors.

### 2.4. Cell cultures

The 2D HepaRG cultures were used as a benchmark to compare with the 3D hydrogel cell cultures. HepaRG cells were cultured in 2D format as described previously [23,24]. Shortly, HepaRG cells were plated either at progenitor state to study the differentiation process or at differentiated state (obtained with DMSO treatment) to study the maintenance of the differentiation. Undifferentiated progenitor cells were seeded at low-density ( $2.6 \times 10^4$  cells/cm<sup>2</sup>) and differentiated at high-density ( $45 \times 10^4$  cells/cm<sup>2</sup>). The cell cultures were placed to the different dishes depending on the end-point analyses (Table 1). The medium volume was set to be 400 μl/cm<sup>2</sup> in low-density cultures and 600 μl/cm<sup>2</sup> in high-density cultures, hereby representing the equal total volumes with 3D hydrogel cultures.

The HepaRG cells were embedded in 3D NFC and HG hydrogels. Undifferentiated cells were seeded at low-density (one million cells/ml of hydrogel) and differentiated at high-density (nine million cells/ml of hydrogel). NFC hydrogel-based 3D cell cultures were prepared by mixing the HepaRG cell suspension with 1.7 wt% NFC hydrogel to achieve 1 wt% hydrogels with desired cell density. The mixing was performed by pipetting up and down with low-retention pipette tips (TipOne®, Starlab Group). HG hydrogel-based 3D cell cultures were prepared according to the manufacturer's instructions (Glycosan Biosystems). Briefly, the cells were mixed with HG solutions followed by the gelification at 37 °C in an atmosphere containing 5% CO<sub>2</sub>. The cell cultures were placed to the different dishes depending on the end-points analysis (Table 1). The volume of the hydrogel cell cultures was set to be 200 μl/cm<sup>2</sup> in each dish. The medium volume (on the top of the hydrogel) was set to be 200 μl/cm<sup>2</sup> for low-density cultures and 400 μl/cm<sup>2</sup> for high-density cultures, hereby representing the equal total volumes with 2D cultures.

The low-density cultures were maintained with the standard HepaRG growth medium and the high-density cultures with HepaRG differentiation medium supplemented with DMSO [23]. The equal volume of the medium was renewed daily both from the 2D and 3D hydrogel cultures (2/3 of the medium volume in the hydrogel cultures). The cell cultures were maintained at 37 °C in an atmosphere containing 5% CO<sub>2</sub>.

### 2.5. Microscope analysis of cell growth

Cell cultures were monitored by phase contrast microscopy (Leica DM IL LED) and images were taken over the time. The average diameter of spheroids was defined from the phase contrast images with LAS EZ software (Leica Microsystems) using the distance line facility. Minimum of 10 spheroids were measured to attain the average size.

### 2.6. Cell viability

The mitochondrial metabolic activity of the cells was determined using oxidation-reduction indicator, resazurin (alamarBlue® Cell Viability Reagent, Invitrogen), 1/10 of the co-volume of medium and hydrogel. To ensure the mixing of the indicator in hydrogels the culture plates were gently shaken (150 rpm) for 10 min both in the beginning and the end of the incubation (Heidolph incubator 1000 equipped with Titramax 1000 shaker). After exposure of 3 h to resazurin at 37 °C in 5% CO<sub>2</sub>, 50 μl of medium was transferred from each culture well to another 96-well plate and the fluorescent metabolite of resazurin (resorufin) was recorded with a plate reader (Varioskan Flash, Thermo Fisher) using excitation at 560 nm and emission at 590 nm. Three independent experiments of both low-density and high-density cultures were carried out. The mitochondrial metabolic activity of the cells was examined within the same wells as CYP3A4 activity and RT-PCR.

Cell viability was analyzed using LIVE/DEAD® viability/cytotoxicity kit (Molecular Probes™). In this case, 0.5 μM calcein-AM and 2 μM ethidium homodimer-1 were added to the cultured cells in Hank's balanced salt solution (HBSS). The conversion of

non-fluorescent calcein-AM into fluorescent calcein and the binding of ethidium homodimer-1 (EthD-1) to DNA were followed with Leica TCS SP5 II HCS A confocal microscope equipped with HCX PL APO 20×/0.7 Imm Corr (water) objective and QD 405/488/561/635 beam splitter. Within 30 min after addition of the reagents, the fluorophores were excited with a 488 nm/35 mW argon laser, and emission was acquired with HyD detectors at 500–550 nm (calcein) and 620–700 nm (EthD-1). The confocal images were analyzed with Imapris 7.4 program (Bitplane) and either slice or surpass images were constructed. Minimum of three independent low-density and high-density cultures were analyzed.

### 2.7. Real time polymerase chain reaction (RT-PCR)

The transcript levels of regulative and functional genes in 3D hydrogel cultures and standard 2D cultures were determined at various times after cell seeding. The expression levels were compared to the human liver tissue. Hydrogel cultures and liver tissues were disrupted with TissueRuptor (Qiagen). Total RNA was extracted from liver samples with TRI reagent (Sigma) or RNeasy (Qiagen), and treated with DNase I (Fermentas) according to the manufacturer's instructions. RNA extraction from the 2D and 3D cell cultures was performed with RLT buffer and spin technology (RNeasy Mini kit, Qiagen). RNA extraction was performed from the same RLT lysates as DNA measurements (see Paragraph 2.8.). The concentration and purity of aqueous RNA solutions was analyzed with NanoDrop™ spectrophotometer (ND-1000 V3.7.0, Thermo Scientific). Additionally, quality of RNA from human liver tissues was analyzed by determining the RNA Integrity Number (RIN) with RNA 6000 nano kit and 2100 Bioanalyzer (Agilent). The samples with RINs greater than five were selected for reverse transcription. cDNA was prepared with RevertAid H minus first strand cDNA synthesis kit (Fermentas, Life technologies) according to the manufacturer's RT-PCR protocol in 20 µl volumes using both oligo dT18 primers (1 µl/reaction) and random hexamer primers (0.2 µl/reaction).

Comparative C<sub>T</sub> experiment was performed in 20 µl reaction volume containing Fast SYBR® Green master mix (Applied Biosystems, Life Technologies), 5 ng or 10 ng of cDNA and 200 nM of each primer set. CYP3A4 primers were designed with Primer3-BLAST [25] and KRT19 with Primer Express® (Applied Biosystems, Life Technologies) (Supplementary Table 1). CycloG and HNF4A [26], ALB [27], MDR1 and MRP2 [28] primers have been designed and published previously (Supplementary Table 1). The primers were synthesized by solid phase phosphoramidite (PA) chemistry followed by reversed phase chromatography (RPC) purification (Oligomer Oy, Helsinki, Finland).

The relative quantity of target nucleic acid sequence in samples of three independent experiments was determined with StepOnePlus™ instrument (Applied Biosystems) using Fast mode (95 °C for 20 s, followed by 40 cycles of 3 s at 95 °C, and 30 s at 60 °C). The specificity of amplified targets was validated by melting curve analysis (15 s at 95 °C, 60 s at 60 °C, and 15 s at 95 °C). To determine  $\Delta C_T$  ( $C_{T \text{ target}} - C_{T \text{ reference}}$ ), the expression of the target gene was normalized to expression levels of reference gene (cyclophilin G) within the same sample. Then  $\Delta C_T$  Expression was calculated by using  $2^{-\Delta C_T}$  method and the actual amplification efficiency of each primer pair. Finally to compute the comparative expression of each gene in HepaRG cultures, the  $\Delta C_T$  expression was normalized to the  $\Delta C_T$  expression in the human liver samples (cDNA mixture from four human donors).

### 2.8. CYP3A4 activity

The activity of the most abundant cytochrome P450 isoform, CYP3A4, in HepaRG cells was studied with P450-Glo™ CYP3A4 assays (Promega) containing luciferin isopropyl acetate (luciferin-IPA). Luciferin-IPA is metabolized by CYP3A4 to release luciferin [29], which can be quantified by luminescence. Water volume of the hydrogels was taken into account when the cell cultures were exposed at 3 µM luciferin-IPA for 60 min at 37 °C in 5% CO<sub>2</sub>. To ensure the mix in hydrogels the culture plates were shaken gently (150 rpm) during the first and the last 10 min periods of the incubation (Heidolph incubator 1000 equipped with Titramax 1000 shaker). At the end of incubation period, 50 µl of substrate solution from each well was removed, placed into a white 96-well plate, and 50 µl of firefly luciferase (Luciferin Detection Reagent, Promega) was added to induce luminescence production. After 20 min at RT, the luminescence was recorded with a plate reader (Varioskan Flash, Thermo Fisher Scientific). The luminescence intensity and hereby the CYP3A activity were normalized to the genomic DNA content of each culture. Three independent experiments of both low-density and high-density cultures were carried out. After CYP3A4 activity analysis the same culture wells were examined for mitochondrial activity and RT-PCR.

### 2.9. CYP3A4 induction

In order to determine influence of 3D culture conditions on the regulatory pathways involved in HepaRG cells, the cells were exposed to prototypic CYP inducers. The activity of the CYP3A4 was assayed. Differentiated HepaRG cells were seeded in NFC and HG hydrogels at 9 million cells/ml of hydrogel and the standard 2D high-density cultures were created by seeding at  $0.45 \times 10^6$  cells/cm<sup>2</sup> [23,30]. During the first 24 h, the cell cultures contained differentiation medium that was changed to DMSO-free medium for the following 72 h. This was done to remove the induction effects of DMSO. On the fourth culture day, dexamethasone (100 µM and

250 µM), phenobarbital (0.2 mM and 1 mM), rifampicin (5 µM and 20 µM) and DMSO (0.5% and 2%) were introduced to the cultures and 0.5% DMSO was used as a vehicle control. The medium with inductor (above the hydrogel) was renewed daily during the 48 h of induction. During the sixth culture day, CYP3A4 activity was analyzed (see CYP3A4 activity chapter). Prior to the analysis, the cell cultures were washed once with 1 × dPBS buffer to remove inductor before adding the luciferin-IPA. The viability of the cultures was analyzed with resazurin (see paragraph Cell viability). Three independent experiments were performed. Each experiment contained triplicate wells per each inducer concentration.

### 2.10. Quantification of genomic DNA

Genomic DNA was quantitated with Quant-iT™ PicoGreen dsDNA assay kit (Molecular probes, Invitrogen). At first, the cell cultures were washed with dPBS. Hydrogel cultures were washed and ruptured by pipetting up and down with dPBS followed by centrifugation (2500 G 5 min). After dPBS removal the cultures were lysed in RLT buffer (RNeasy Mini kit, Qiagen). Additionally hydrogel cultures were disrupted with TissueRuptor (Qiagen) to release the nucleotides from the gel and centrifuged (3000 G 5 min) to remove the hydrogel. Then, the RLT cell lysates were diluted 1:20 with autoclaved milliQ water, 5 µl of each diluted sample and standard were pipetted into DNA-free black 96-well plate (Greiner bio-one), and 100 µl of PicoGreen (diluted 1:100) was added to the wells. The final buffer concentration of 1:400 in the analysis is known to be compatible with the PicoGreen signal [31]. After 5 min incubation at RT the emission of dsDNA samples at 520 nm was recorded with fluorometer (Varioskan Flash, Thermo). Readings from samples were compared to 1–500 ng/ml of control dsDNA provided with kit. Samples from three independent experiments of both low-density and high-density experiments were analyzed. Each lysate was analyzed as triplicate.

### 2.11. Cell morphology and protein localization

Structural polarity of the HepaRG cultures was analyzed by fixing the cell cultures in 4% paraformaldehyde for 15 min at 4 °C. After washing with PBS, the cells were permeabilized with 0.1% Triton X-100 for 15 min and subsequently incubated overnight with a blocking buffer (10% goat serum and 0.2% BSA in PBS) at 4 °C. Then, the cultures were incubated with a primary antibody, anti-MDR1 (1:100, Sigma P7965) or anti-MRP2 (1:300, Abcam ab3373) (diluted in 5% goat serum in 1 × PBS buffer) overnight at 4 °C in a humidified chamber. After washing unbound primary antibody, samples were incubated with goat anti-mouse or goat anti-rabbit antibody conjugated with Alexa Fluor 488 (Invitrogen, diluted 1:200 in 5% goat serum in PBS buffer) for 4 h at RT in a humidified chamber. The cultures were washed with 1 × PBS (four times for an hour) and 1 µg/ml Hoechst 33258 (Sigma–Aldrich, bis-benzimide) together with Alexa Fluor 594-labelled phalloidin (Invitrogen, diluted 1:100 or 1:50 in 1 × PBS buffer) was placed and held for overnight to visualize the nuclei and cellular distribution of the filamentous actin (F-actin) cytoskeleton, respectively.

For immunostaining of the cells in HG hydrogel, the cultures were fixed in 4% paraformaldehyde overnight at 4 °C, dehydrated by passing the hydrogel through a series of increasing alcohol concentrations (50% overnight at 4 °C, 70% for 30 min at RT, 94% for 30 min at RT, 99.5% for 15 min at RT), treated with xylene for 60 min at RT, and filled with paraffin by embedding in hot paraffin for 60 min in Tissue-Tek® TEC™ tissue embedding center (Sakura Finetek Europe). After paraffin was cooled to become solid, the culture was cut in 5–20 µm sections by microtome. The sections on objective glasses were deparaffinized with xylene washes (6 × 10 min) and decreasing alcohol concentrations (99.5% for 3 × 3 min, 94% for 2 × 3 min, 70% for 1 × 3 min, and 50% for 1 × 3 min, all at RT). After cold water wash, antigens were retrieved by boiling in sodium citrate buffer for 5–20 min. The culture sections were washed in TBS buffer with 0.025% Triton X-100, and blocked in 10% goat serum with 0.2% bovine serum albumin in TBS buffer for 2 h or overnight. Staining of proteins and imaging was performed as for the whole mount cell cultures. As exception the actin filaments were stained in uncut HG cultures since phalloidin is not compatible with paraffin embedding.

Stained samples were protected with an antifade reagent (Prolong gold, Invitrogen) and analyzed with a confocal microscope (Leica TCS SP5 with Leica DM5000 upright microscope, HCX APO 63×/1.30 (glycerol) objective and TD 488/561/633 beam splitter). Images were acquired via three channels (430–525 nm, 500–550 nm and 600–700 nm) excited with laser diode 405 nm/50 mW, laser OPSL 488 nm/270 mW, and DPSS 561 nm/20 mW. The confocal images were analyzed with Imapris program (Bitplane) and either slice or surpass images were constructed. The possible deconvolution was done with AutoQuant X program (MediumCybernetics).

### 2.12. Functional polarity

Hepatobiliary transport was investigated with fluorescein diacetate, a marker of efflux transport in hepatocytes [32,33]. Fluorescein diacetate enters the cells passively and undergoes esterase-mediated hydrolysis. Polar fluorescent metabolite, fluorescein, will be entrapped in the cells unless it is actively transported from the cells into the canalicular space. The HepaRG cultures in Nunc™ chambered coverglass slides were exposed to fluorescein diacetate at a final concentration of 10 µM for 5 min at 37 °C in 5% CO<sub>2</sub> and washed with HBSS. Cell-permeable DNA probe

Draq5™ (Biostatus Limited) was placed to cultures in HBSS buffer at 30–60  $\mu\text{M}$  final concentrations. The cells were incubated 30 min at 37 °C in 5%  $\text{CO}_2$  to get nuclei stained after which observed with a Leica TCS SP5 II HCS A confocal laser scanning system with Leica DMI6000 B inverted microscope, HCX PL APO 20 $\times$ /0,7 (water) objective, QD 405/488/561/635 beam splitter and incubator box with air heater system (Life Imaging Services). The fluorophores were excited with lasers Argon 488 nm/35 mW and HeNe 633 nm/12 mW. Emission was acquired at 500–550 nm (fluorescein) and 650–750 nm (Draq5™). The transmitted light was also collected. The confocal images were analyzed with Imaris 7.4 program (Bitplane) and either slice or surpass images were constructed.

### 3. Results

#### 3.1. Cell growth and viability

HepaRG cells formed multicellular spheroids in NFC and HG hydrogels during the first culturing days (Fig. 1A and B). The number of spheroids in NFC and HG hydrogel images cannot be directly compared due to the differences in the optical and structural properties of the hydrogels (Fig. 1A and B). The size of the spheroids exceeded the size of a single HepaRG cell (circa 13  $\mu\text{m}$  in diameter) already during the first day (Fig. 1A and B), and they reached the full size (circa 40  $\mu\text{m}$  in diameter) within a week. NFC hydrogel cultures of progenitor state (low-density) and

differentiated (high-density) HepaRG cells resulted in similar spheroids sizes (about 40  $\mu\text{m}$  in diameter). The spheroids of the high-density NFC cultures appeared to be less organized (Fig. 1B) when compared to the low-density NFC cultures (Fig. 1A). The spheroids in high-density HG retained the same size during the six days of culture (Fig. 1B) and were smaller than in the low-density HG cultures (Fig. 1A).

Based on the DNA quantification and mitochondrial activity, the low-density HepaRG cells exhibited slow growth within the hydrogels (Figs. 2A and C). No proliferation was seen in the high-density cultures and the content of DNA in fact decreased in NFC and 2D cultures. On the first culture day, the different DNA content between the 2D, NFC and HG cultures results from the different numbers of the seeded cells (Fig. 2A and B).

Overall, the mitochondrial activity was lower in high-density than in low-density cultures (Fig. 2C and D). Mitochondrial activity was higher in 2D and NFC cultures than in the HG cultures (Fig. 2C and D). Nonetheless, the live/dead staining studies indicated that all the cultures were viable at both seeding densities (Fig. 3). HepaRG spheroids were viable for at least two weeks (Fig. 3). The dead cells were mainly the singular cells outside of the spheroids (Figs. 1 and 3).

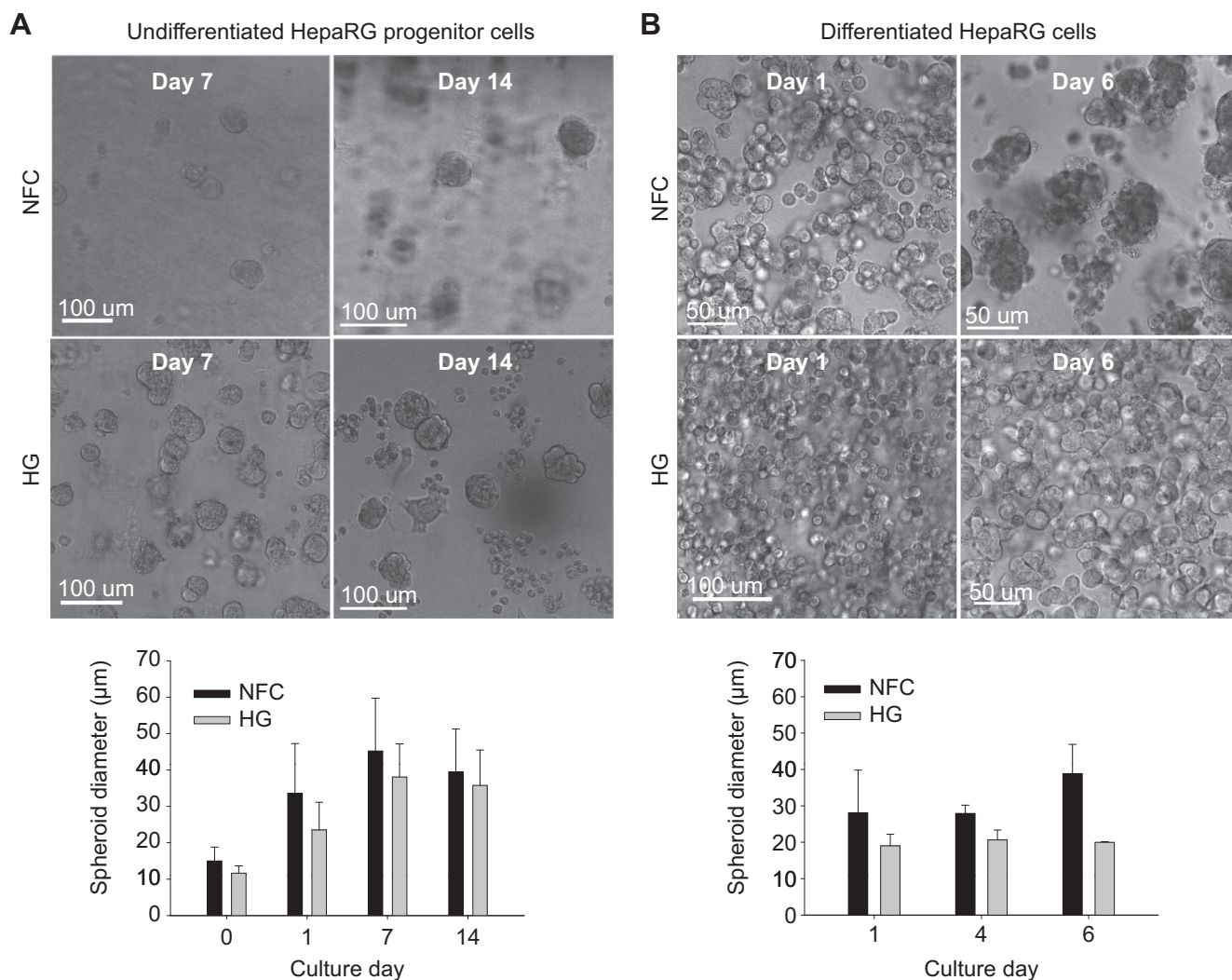


**Fig. 1.** Growth of HepaRG cells upon seeding in nanofibrillar cellulose (NFC) and hyaluronan-gelatin (HG) hydrogels. The HepaRG cells formed spherical aggregates, spheroids, in the hydrogels when they were embedded A) as hepatic undifferentiated progenitors at density of 1 million/ml (low-density) and B) as differentiated cells at density of 9 million/ml (high-density). The spheroids grew more in size when the cells were seeded at low-density compared to cultures seeded at high-density.

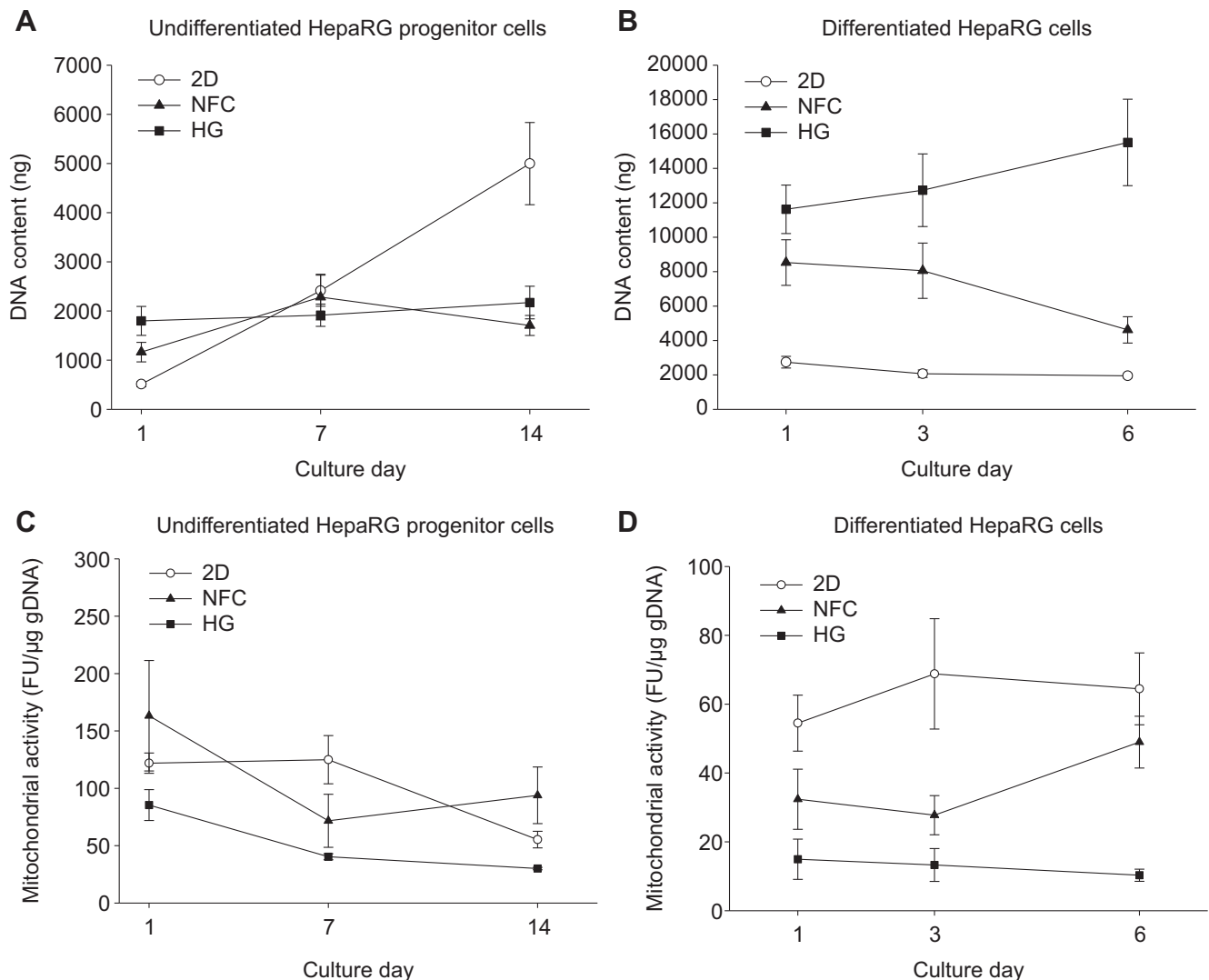


**Fig. 2.** Proliferation and viability of HepaRG cells were determined based on the DNA content and mitochondrial activity. A) Compared to the 2D plated cells the proliferation of the low-density progenitor cells in the hydrogels was remarkably slower. B) At high-density cultures, the differentiated cells did not proliferate. D) The mitochondrial activity was generally lower in high-density than C) in low-density cultures. The results show the mean of three independent cell culturing experiments. Error bars indicate standard error. 2D, two-dimensional; HG, hyaluronan-gelatin; NFC, nanofibrillar cellulose.

### 3.2. Expression of regulating and functional genes

Expression levels of hepatic nuclear factor 4 $\alpha$  (HNF4A), albumin (ALB), CYP3A4 and keratin 19 (KRT19) transcripts were studied to assess the differentiation of the HepaRG cells towards hepatocytes or cholangiocytes. Additionally efflux transporters MDR1 (P-gp, ABCB1) and MRP2 (ABCC2) were analyzed as markers of hepatic differentiation and drug transport capacity.

HepaRG showed differentiation towards hepatocyte phenotype in all tested microenvironments after low-density seeding (Fig. 4A). The upregulation of HNF4A, ALB and CYP3A4 demonstrates the differentiation to hepatocyte direction. Furthermore, down-regulation of the cholangiocyte marker KRT19 in low-density NFC and 2D cultures shows that the differentiation proceeds towards hepatocyte phenotype, not cholangiocyte (Fig. 4A). No down-regulation of KRT19 in HG cultures was detected, but the initial expression level of KRT19 in HG cultures was lower than in 2D and NFC cultures. Expression of HNF4A was higher in HG cultures than in 2D and NFC cultures suggesting higher differentiation state of the cells (Fig. 4A). The transcript of CYP3A4 was not detectable in

standard 2D cultures during the first week of culture. However, in NFC and HG hydrogel cultures the mRNA of CYP3A4 was seen after culture day one and the expression levels of human liver were reached within a week of cell culture.

When differentiated HepaRG cells were seeded in NFC at high-density, KRT19 was upregulated and the hepatic differentiation markers; CYP3A4, HNF4A, ALB, MDR1 and MRP2 were down-regulated when compared to HG and 2D cultures (Fig. 4B). Expression of KRT19 mRNA was lower in 2D and HG microenvironments than in NFC, which showed high KRT19 expression during the whole culturing time. Furthermore, the expression of KRT19 was remarkably higher in HepaRG cells than in human liver. CYP3A4 mRNA expression in high-density 2D and HG cultures was comparable to human liver tissue or even higher (Fig. 4B). Instead, high-density NFC cultures expressed less CYP3A4 mRNA than the human liver.

Expression of the efflux transporters, MDR1 and MRP2, was higher in all the HepaRG cultures (both 2D and 3D cultures) than in the human liver tissue (Fig. 4). In low-density cultures, HG hydrogels increased the expression of MDR1 and MRP2 efflux transporter

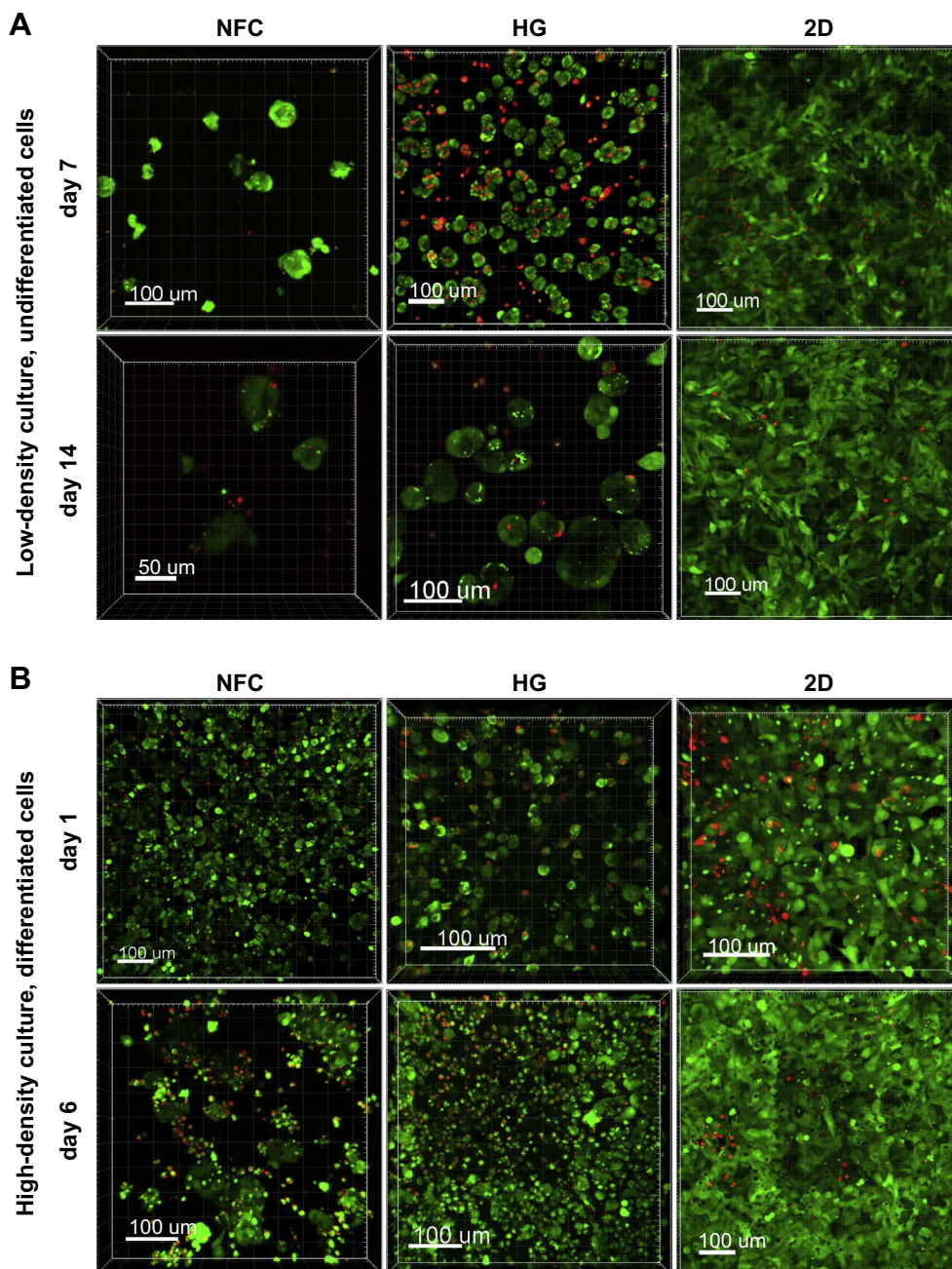


**Fig. 3.** Viability of HepaRG cells seeded in nanofibrillar cellulose (NFC) and hyaluronan-gelatin (HG) hydrogels and on standard polystyrene dish (2D) was measured with LIVE/DEAD<sup>®</sup> viability/cytotoxicity kit. The cytosols of viable (green) and nuclei of dead (red) cells are stained. A) Low-density progenitor cultures were investigated after 1 and 2 weeks of culture, and B) high-density differentiated cell cultures at culturing days 1 and 6. (For interpretation of the references to colour in this figure legend, the reader is referred to the web version of this article.)

transcripts. In the case of high-density cultures, the highest expression of efflux transporters was seen in the 2D cultures.

### 3.3. CYP3A4 activity

CYP3A4 enzyme activity of the HepaRG cells was higher in the NFC embedded cells than in the HG and 2D cultures (Fig. 5A). In the beginning of the culture the activity was equal in NFC and 2D cultures, but the activity of the NFC cultures increased in average 4-fold during the two weeks of culture while the activity of 2D cultures remained at the same level. The 4-fold increase took place also in HG hydrogel but the activity in the HG cultures was very low.

CYP activity of differentiated cells (Fig. 5B) was higher in the 2D environment than in the hydrogels, and the activity was circa 100-fold higher in NFC than in HG cultures.

### 3.4. CYP3A4 induction

CYP3A4 activity was inducible in HepaRG cells cultured in NFC and HG hydrogels and 2D environment (Supplement Fig. 1). The relative levels of enzyme induction were similar in the 3D hydrogel-based cell cultures and in the 2D cell cultures. The prototypical CYP3A4 inducers rifampin and phenobarbital and non-specific

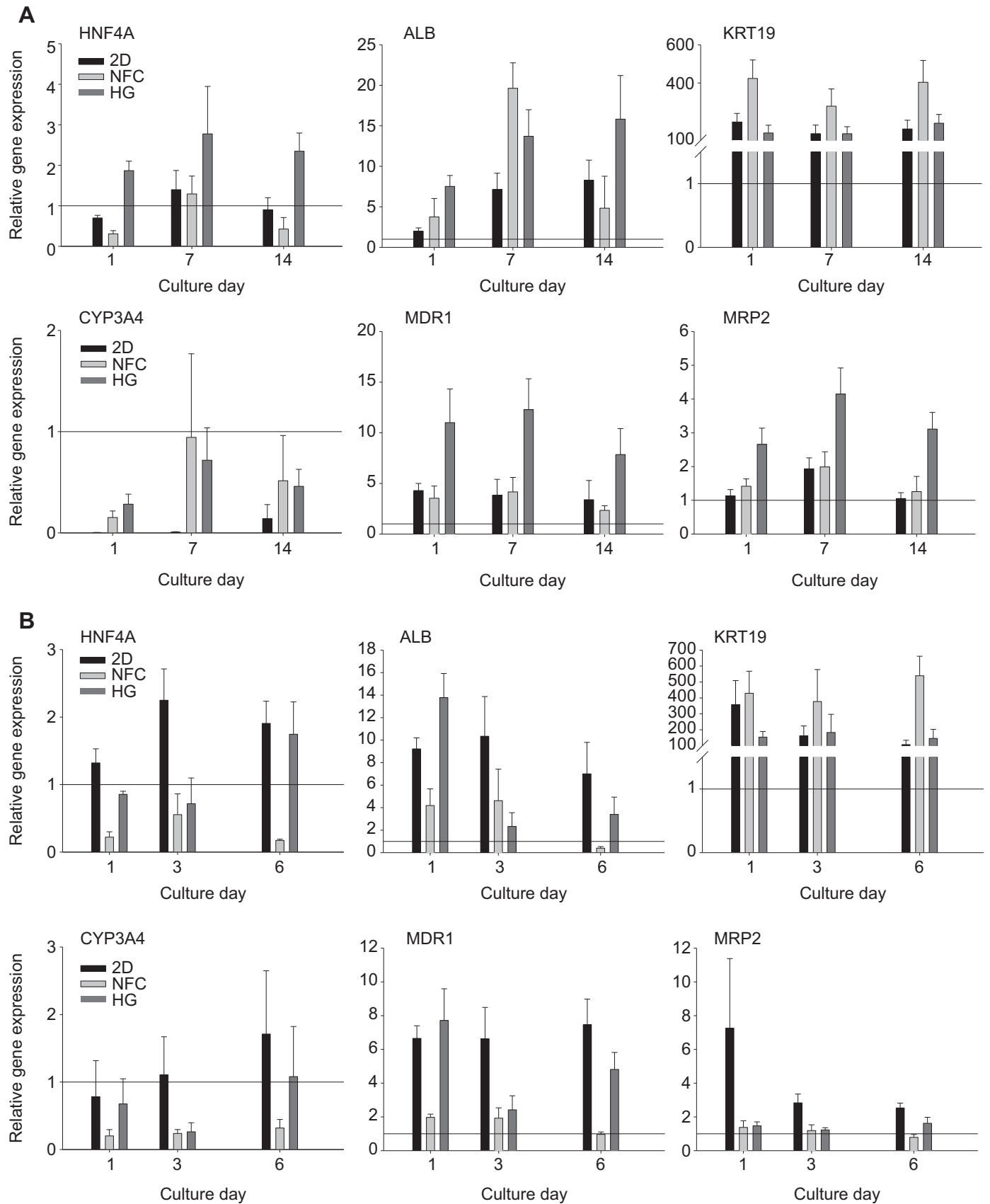


**Fig. 4.** Comparative expression of hepatic genes in human liver and in HepaRG cells seeded A) undifferentiated at low-density and B) differentiated at high-density. Results are expressed as percentage compared to human liver (the control line). Results express the mean of three independent cell culture experiments. Error bars indicate standard error. ALB, Albumin; CYP3A4, Cytochrome P450 3A4; HG, hyaluronan-gelatin; HNF4A; hepatic nuclear factor 4A; KRT19, keratin 19; MDR1 (ABC1) ATP-binding cassette sub-family B member 1 transporter; MRP2 (ABC2) ATP-binding cassette sub-family C member 2 transporter; NFC, nanofibrillar cellulose.

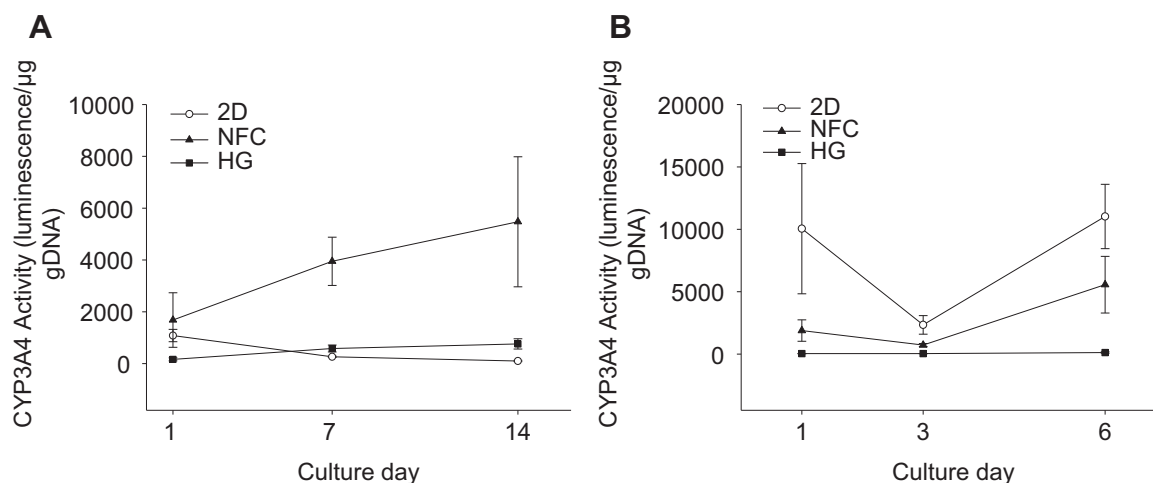


**Fig. 5.** CYP3A4 enzyme activity of HepaRG cells upon seeding in nanofibrillar cellulose (NFC) and hyaluronan-gelatin (HG) hydrogels and on 2D plates. A) Hydrogel culturing enriched the CYP3A4 mediated metabolism when cells were embedded as hepatic progenitors at low-density. B) In the beginning of the high-density culture, the activity of differentiated cells decreased but recovered later in NFC and 2D environments. Results express the mean of three independent cell culturing experiments  $\pm$  standard error.

gene inducer DMSO induced the CYP activity, but dexamethasone did not.

### 3.5. Formation of bile canaliculi in the cell cultures

The characteristic markers of the canalicular plasma membrane were studied by staining the F-actin and the canalicular resident membrane transporters, MRP2 and MDR1 (Fig. 6). The accumulation of F-actin and the localization of MRP2 and MDR1 on the canalicular membrane were seen in all low-density HepaRG cultures (Fig. 6A). All spheroids in the NFC or HG hydrogels showed either several canalicular structures (Fig. 6A) or the canaliculi that stretched through the spheroid (Supplementary Fig. 2). Again, in the 2D cultures, the stained canalicular structures were located in the hepatocyte phenotype areas.

Canalicular structures were also formed in the high-density cultures (Fig. 6B). MRP2 was localized at canalicular membranes in all high-density cultures, but MDR1 localization was not detected in the high-density spheroids.

### 3.6. Functional polarity

Accumulation of fluorescein into the round vesicle-like compartments between adjacent cells was evident in the 3D low-density spheroid cultures and 2D cell cultures (Fig. 7A, Supplementary Animation 1). In the standard 2D cultures, fluorescence accumulated in the areas that show hepatocyte-like phenotype. Flat biliary-like epithelial cells remained green longer time than the granular hepatocyte-like cells and they did not form vesicle structures. High-density cultures presented less vesicle structures than low-density cultures (Fig. 7B). Efflux of fluorescein was not seen in the single cells, outside of the spheroids. These single cells remained green in the NFC cultures, demonstrating that the efflux transport was associated with the formation of intercellular vesicle compartments (Fig. 7B).

Supplementary data related to this article can be found online at <http://dx.doi.org/10.1016/j.biomaterials.2014.03.020>

Canalicular domain activity was further confirmed with calcein, a MRP2 substrate [34]. This was evident in the live/dead analyses of the cultures. Green calcein staining is normally retained in the cytoplasm of live cells but in this study we saw time-dependent accumulation of calcein in the intercellular canalicular vesicles

(Supplementary Fig. 3). After 20–30 min from calcein introduction to the cultures, the green color in the cytosols became lighter and the fluorescence in the vesicles emerged. The fluorescent vesicle structures were identified both in low-density and high-density cultures, in both 3D hydrogel and 2D cultures. The data (Supplementary Fig. 3) suggests that there are more bile canaliculi-like structures in HG than in NFC cultures.

## 4. Discussion

New organotypic liver cell culture systems are developed with different combinations of tissue engineering techniques, biomaterials and cell types [35]. Continuous cell lines are more practical than primary cells in drug and chemical testing, because they can be frozen and cultured more conveniently. Among continuous cell lines, HepaRG more closely resembles human hepatocytes than HepG2 and many other liver cell lines [6,36], and have been successfully used to predict hepatic pharmacokinetics in humans [6–8] and to analyze toxicity of chemicals [4,5]. However, HepaRG has never been cultured in 3D format in biomaterials. Prior 3D cultures of HepaRG have been generated using bioreactor [8] and hanging-drop technique [37].

Herein, the plasticity of HepaRG liver cells was exploited to evaluate the impact of naturally derived hydrogels, native nanofibrillar cellulose (NFC) and hyaluronan-gelatin (HG), on the phenotype of both undifferentiated HepaRG progenitors and differentiated HepaRG cells. Wood-derived NFC is a promising new material for 3D cell culture. In our previous study [12], NFC and HG were the most promising biomaterials for 3D cell culture and, therefore, they were chosen to this study.

### 4.1. HepaRG growth in 3D hydrogel cultures

HepaRG cells formed spheroids in both NFC and HG hydrogels. The spheroids of low-density progenitor cells had smooth surfaces suggesting that they are better organized than the spheroids of high-density cell cultures. The spheroids were smaller than the HepaRG spheroids that were previously generated in hanging-drops [37]. The high cell viability in hydrogels is in line with previous publications on cell studies in fibrillated cellulose [14,38] and hyaluronan-gelatin gels [21].

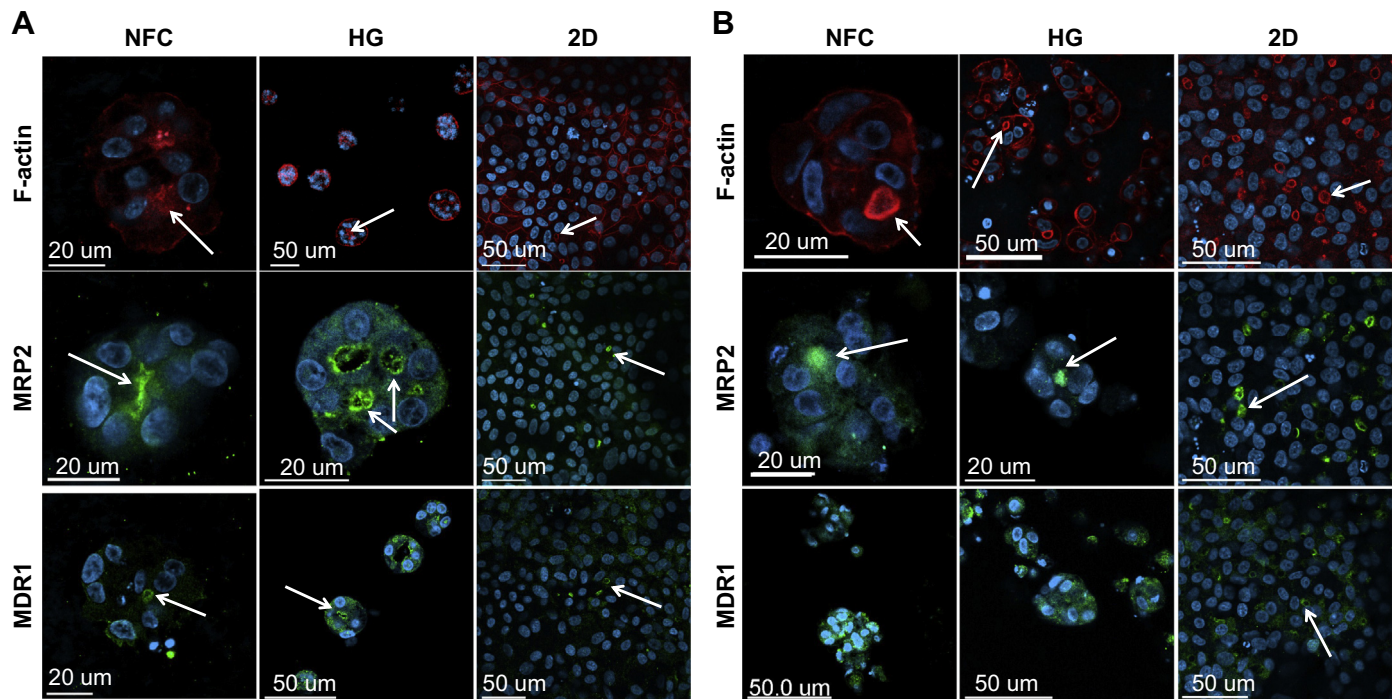


**Fig. 6.** Staining of filamentous actin (F-actin) and hepatobiliary transporters, MRP2 and MDR1, in the HepaRG cultures. Canalicular accumulation of F-actin was visible in both A) low-density and B) high-density cultures. A) In low-density cultures initiated with undifferentiated cells, both MRP2 and MDR1 are located the apical side (bile canalicular side). B) MRP2 was correctly localized in canalicular membrane in all high-density hydrogel cultures, but MDR1 localization to canalicular cell side was not observed in the high-density hydrogel cultures. The cells were cultured for 14 or 3 days, followed by immunostaining either with anti-MRP2 and anti-MDR1 antibodies labeled with Alexa fluor 488 (green). F-actin and nuclei were visualized with Alexa fluor 594-phalloidin (red) and Hoechst 33258 (blue), respectively. HG, hyaluronan-gelatin; MDR1 (ABCB1), ATP-binding cassette sub-family B member 1; MRP2 (ABCC2), ATP-binding cassette sub-family C member 2; NFC, nanofibrillar cellulose. (For interpretation of the references to colour in this figure legend, the reader is referred to the web version of this article.)

The decreased proliferation is typical for the cells in 3D hydrogels, and it may be due to the effects of the mechanical strength and hydrogel chemistry on the cell phenotype [39,40]. Interestingly, HG hydrogel hosts similar biochemical signals than the ECM in the liver but NFC is a polysaccharide from plants without any human ECM components. Also the internal structure of these hydrogels is different: HG is a strong hydrogel with covalent cross-links, while the NFC hydrogels are physically cross-linked by hydrogen bonds between nanofiber flocs [41]. The viscoelastic properties of NFC and HG hydrogels resemble each other: the shear elastic modulus of 0.4% HG hydrogel is 70–95 Pa [22] while the storage modulus  $G'$  of 1% NFC hydrogel is close to 100 Pa [42]. Not surprisingly, the cell proliferation was not seen in the high-density cell cultures. The high cell number and the hydrogel environment limit the proliferation [24,39,40].

#### 4.2. Expression of differentiation biomarkers

RT-PCR assay demonstrates that HepaRG differentiates in the NFC and HG hydrogels since the mRNA levels of CYP3A4 and ALB increased during the two weeks of culture. The elevated HNF4A, ALB, CYP3A4, MDR1 and MRP2 expression in 3D HG cultures suggests more prominent hepatocyte-like phenotype compared to the 2D cultures. NFC hydrogels induced the expression of CYP3A4 and ALB but also the upregulation of KRT19 transcript was seen. Interestingly, CYP3A4 expression was remarkably higher in low-density 3D hydrogel cultures than in the 2D cultures, and was nearly the level of human liver. The expression of CYP3A4 mRNA was not even detectable during the first week of the 2D cultures that is in line with the previous data [30].

RT-PCR data on HNF4A implies that the differentiation level of differentiated high-density HepaRG cell cultures decreased after seeding in the hydrogels. The loss of the hepatocyte differentiation markers was milder in the HG than in the NFC cultures. The mRNA expression of CYP3A4 in high-density 2D and HG cell cultures was comparable to the human liver, whereas in NFC the expression was clearly lower.

The expression of KRT19 transcript was higher in HepaRG cells, both in 2D and 3D hydrogel cultures, than in the human liver. This shows the bipotent character of HepaRG and indicates increased presence of cholangiocyte-like cells in the HepaRG cultures compared to the human liver.

#### 4.3. CYP3A4 activity and induction

The higher CYP3A4 activity in the hydrogel cultures than in the standard 2D cultures shows that both NFC and HG hydrogels expedite the differentiation of HepaRG progenitor cells. We propose that the hydrogel microenvironments inhibit the proliferative phase [39,40], but the hydrogel culture accelerates cell differentiation possibly by facilitation of the cell–cell contacts. On the contrary, the high-density cell cultures with differentiated HepaRG cultures showed higher CYP3A4 activity in 2D environment than in 3D NFC and HG hydrogels. Nevertheless, the CYP activity of high cell density NFC cultures was near the activity of high cell density 2D cultures and reached the level of low cell density NFC cultures.

The study on CYP3A4 inducibility demonstrated that induction was in the same range in both the hydrogel and 2D cultures. Thus, 3D culturing in NFC and HG hydrogels did not violate the sensitivity of HepaRG cells to the prototypical CYP inducers. The induction of luciferin-IPA metabolism by rifampicin and phenobarbital was

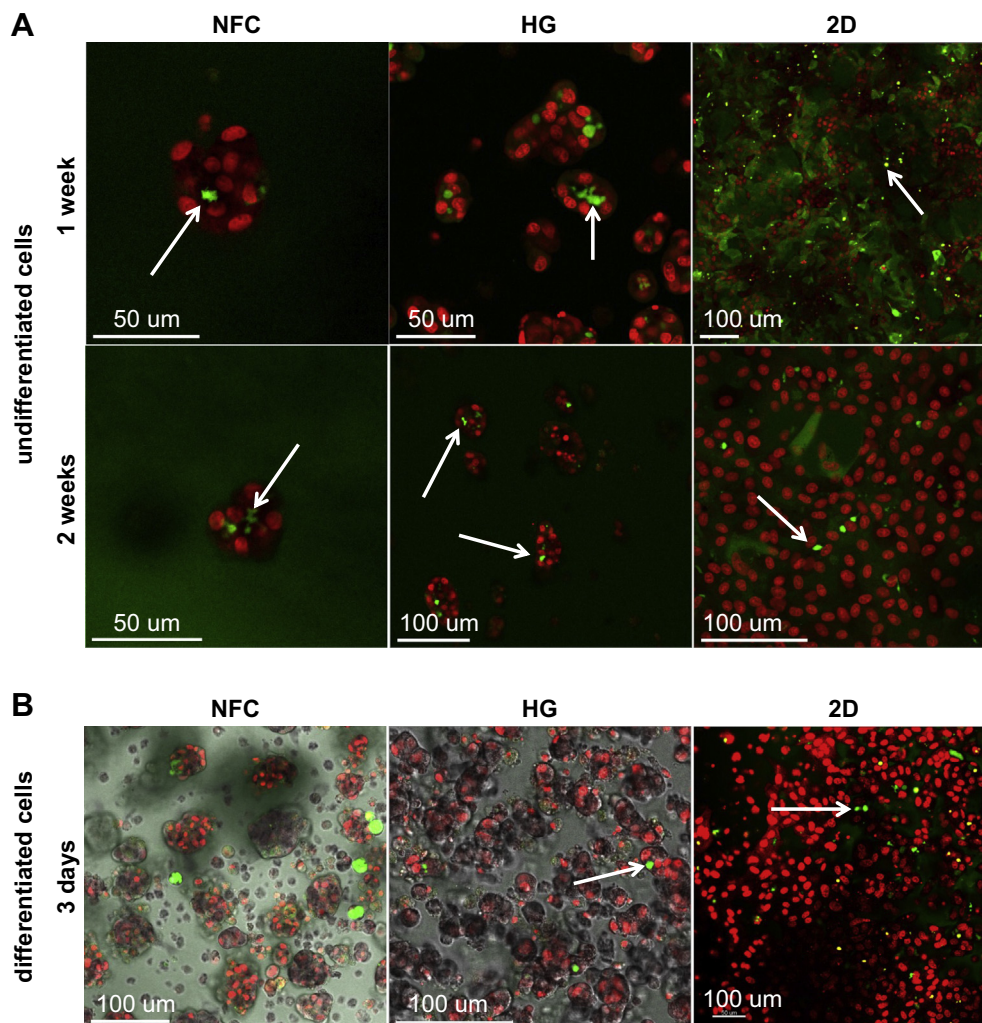


**Fig. 7.** Canalicular transport of fluorescein in HepaRG cultures demonstrates the correct localization and function of hepatobiliary transporters. The living cells were incubated with fluorescein diacetate that enters the HepaRG cells, is cleaved by intracellular esterases to fluorescein (green), and is excreted into the bile canaliculi-like structures by hepatobiliary transporters. Fluorescein does not diffuse from the cells without active transport. A) The accumulation of fluorescent fluorescein (green) into intercellular vacuoles was detected in all the low-density cell cultures and B) in 2D and HG cultures that were seeded at high-density. Accumulation demonstrates correct localization and function of hepatobiliary transporters in HepaRG spheroids. Nuclei were stained with Draq5™ (red). 2D, two-dimensional; HG, hyaluronan-gelatin; NFC, nanofibrillar cellulose. (For interpretation of the references to colour in this figure legend, the reader is referred to the web version of this article.)

consistent with the induction measured earlier in HepaRG cultures [4,8,43]. In this study, dexamethasone induction of CYP3A4 activity was detected neither in 2D nor 3D hydrogel HepaRG cultures, but earlier study with 2D HepaRG culture has reported 2-fold induction at mRNA when treated with dexamethasone [7]. Although CYP activity of HG cultures was low the CYP3A4 induction was in same range as seen in 2D and NFC cultures.

#### 4.4. Expression, localization and activity of canalicular efflux transporters

In low-density NFC and 2D cultures, the expression of MDR1 and MRP2 transcripts were in the same range, whereas the expression was higher in the HG cultures than in the NFC and 2D cultures. On the contrary, high-density 2D cultures expressed transporters at higher level than the NFC and HG cultures. Altogether, the expression of MDR1 transcript was higher in HepaRG cells, both in 2D and hydrogel cultures, than in the human liver, which is in agreement with the previous findings [36,44]. The expression of another efflux transporter, MRP2, was either at same level or higher

than in the human liver, which agrees with a previous study [36] but contrasts with some other findings [5,44].

The canalicular accumulation of F-actin in the spheroids of both low-density and high-density cultures indicates *in vivo*-like polarity and formation of bile canaliculus. Bile canaliculus formation was confirmed in the expression and functional studies. The canalicular localization of MRP2 and MDR1 resembles the situation *in vivo* and suggests that the cells have hepatocyte-like phenotype in the spheroids. In the 2D cultures, MRP2 and MDR1 were located solely in the granular hepatocyte-like cells as previously published [8,37].

Transport of fluorescein and calcein into the canalicular vesicles suggests that the MRP2 is functionally active in the bile canalicular structures of HepaRG spheroids. Fluorescein is a substrate for canalicular efflux transporter MRP2 [32,33] and bile salt export pump (BSEP) [45], whereas calcein is a substrate for MRP2 [34], but not for the other liver canalicular efflux transporters MDR1 [46] and BCRP [47]. Previously, MRP2 activity in HepaRG cells has been discovered with fluorescein, 5 (and 6)-carboxy-2',7'-dichloro-fluorescein, and glutathione-methylfluorescein [5,24,37]. Both infrequent bile canaliculi structures and lack of MDR1 staining in

**Table 2**  
The Overall summary of results.

	HepaRG progenitor cells			HepaRG differentiated cells		
	2D	3D NFC	3D HG	2D	3D NFC	3D HG
Cell proliferation	+++	+	+	–	–	–
Mitochondrial activity	+++	+++	++	++	+	+
Cell viability staining	+++	+++	+++	++	++	++
Albumin mRNA expression	++	+++	+++	++	+	+
CYP3A4 mRNA expression	–	++	++	+++	+	++
CYP3A4 activity	+	++	+	+++	++	+
MDR1 and MRP2 mRNA expression	++	++	+++	+++	+	++
MDR1 and MRP2 localization	+	+	+	+	–	–
MDR1 and MRP2 activity	+	+++	+++	++	+	++

high-density spheroids suggest that the differentiated cells are less polarized than the low-density spheroids.

#### 4.5. Comparison of 2D and 3D (NFC, HG) cell cultures

Table 2 summarizes the results of this study. Compared to high-density cultures of pre-differentiated cells, the low-density cultures result in improved organotypic cell differentiation. Among low-density cultures, the 3D format typically results in improved albumin expression and activity and expression of CYP3A4 and efflux transporters. Overall, NFC and HG showed similar performance as 3D matrices for hepatic progenitor differentiation.

#### 4.6. Potential of 3D HepaRG cell cultures for drug and chemical testing

This study proves that culturing HepaRG cells in hydrogels allows formation of 3D structures toward more organotypic liver tissue model. The improved CYP3A4 activity together with the apicobasal polarity and efflux transporter activity makes HepaRG spheroids interesting for drug and chemical testing. The 3D HepaRG spheroids may be of great value in assessing drug excretion to the bile, efflux transporter-mediated drug–drug interactions and toxicity of chemical compounds. The current 2D hepatocyte cultures do not reach the apicobasal polarity and only the sandwich-cultured hepatocytes are appropriate for the prediction of *in vivo* bile excretion [1,2].

## 5. Conclusions

Improved cell culture models of hepatocytes are needed in the drug discovery, drug development, and chemical testing. Biomaterial (wood-derived nanofibrillar cellulose and hyaluronan – gelatin) hydrogels induced differentiation of continuous HepaRG progenitor cell line to organotypic 3D spheroids with bile duct compartment in the core. The spheroids showed expression of hepatocyte markers, metabolic activity and vectorial molecular transport towards bile duct compartment. Wood-derived nanofibrillar cellulose and hyaluronan-gelatin hydrogels are powerful matrices for 3D hepatocyte spheroid formation. Generation of organotypic hepatocyte cultures from continuous progenitor cell line paves way to improved hepatocyte cultures for drug and chemical testing.

## Acknowledgements

We thank Kimmo Tanhuanpää and Mika Molin from the Light Microscope Unit, University of Helsinki for excellent technical guidance in design and execution of confocal microscopy and image

processing. Eija Koivunen from the Department of Biosciences, University of Helsinki is acknowledged for orientation to the paraffin embedding. Carmen Escopedo-Lucea and Marika Häkli from the Division of Biopharmaceutics and Pharmacokinetics and Centre for Drug Research, University of Helsinki, respectively, are gratefully thanked for the transport and processing of human liver tissues. Antti Laukkanen from UPM New Businesses and Development is granted for valuable comments on the hydrogel properties. Sanna Toivonen from the Molecular Neurology and Biomedicum Stem Cell Center, University of Helsinki is granted for the design of CycloG and HNF4A primers. This work was funded and supported by Tekes-The Finnish Funding Agency for Technology and Innovation (3D-Liver project), EU-FP7 (LIV-ES project, HEALTH-F5-2008-223317), Graduate School of Pharmaceutical Sciences, and Orion-Farmos Research Foundation.

## Appendix A. Supplementary data

Supplementary data related to this article can be found at <http://dx.doi.org/10.1016/j.biomaterials.2014.03.020>

## References

- [1] Abe K, Bridges AS, Brouwer KL. Use of sandwich-cultured human hepatocytes to predict biliary clearance of angiotensin II receptor blockers and HMG-CoA reductase inhibitors. *Drug Metab Dispos* 2009;37:447–52.
- [2] Pedersen JM, Matsson P, Bergstrom CA, Hoogstraate J, Noren A, Lecluyse EL, et al. Early identification of clinically relevant drug interactions with the human bile salt export pump (BSEP/ABCB11). *Toxicol Sci* 2013;136:328–43.
- [3] Noor F, Niklas J, Muller-Vieira U, Heinzle E. An integrated approach to improved toxicity prediction for the safety assessment during preclinical drug development using Hep G2 cells. *Toxicol Appl Pharmacol* 2009;237:221–31.
- [4] Josse R, Aninat C, Glaize D, Dumont J, Fessard V, Morel F, et al. Long-term functional stability of human HepaRG hepatocytes and use for chronic toxicity and genotoxicity studies. *Drug Metab Dispos* 2008;36:1111–8.
- [5] Antherieu S, Chesne C, Li RY, Camus S, Lahoz A, Picazo L, et al. Stable expression, activity, and inducibility of cytochromes P450 in differentiated HepaRG cells. *Drug Metab Dispos* 2010;38:516–25.
- [6] Lubberstedt M, Muller-Vieira U, Mayer M, Biemel KM, Knospel F, Knobloch D, et al. HepaRG human hepatic cell line utility as a surrogate for primary human hepatocytes in drug metabolism assessment *in vitro*. *J Pharmacol Toxicol* 2011;63:59–68.
- [7] Kanebratt KP, Andersson TB. HepaRG cells as an *in vitro* model for evaluation of cytochrome P450 induction in humans. *Drug Metab Dispos* 2008;36:137–45.
- [8] Darnell M, Schreiter T, Zeilinger K, Urbaniak T, Soderdahl T, Rossberg I, et al. Cytochrome P450-Dependent metabolism in HepaRG cells cultured in a dynamic three-dimensional bioreactor. *Drug Metab Dispos* 2011;39:1131–8.
- [9] Salerno S, Campana C, Morelli S, Drioli E, De Bartolo L. Human hepatocytes and endothelial cells in organotypic membrane systems. *Biomaterials* 2011;32:8848–59.
- [10] Skardal A, Smith L, Bharadwaj S, Atala A, Soker S, Zhang Y. Tissue specific synthetic ECM hydrogels for 3-D *in vitro* maintenance of hepatocyte function. *Biomaterials* 2012;33:4565–75.
- [11] Meli L, Jordan ET, Clark DS, Linhardt RJ, Dordick JS. Influence of a three-dimensional, microarray environment on human cell culture in drug screening systems. *Biomaterials* 2012;33:9087–96.
- [12] Bhattacharya M, Malinen MM, Lauren P, Lou YR, Kuisma SW, Kanninen L, et al. Nanofibrillar cellulose hydrogel promotes three-dimensional liver cell culture. *J Control Release* 2012;164:291–8.
- [13] Lou YR, Kanninen L, Kuisma T, Niklander J, Noon LA, Burks D, et al. The use of nanofibrillar cellulose hydrogel as a flexible three-dimensional model to culture human pluripotent stem cells. *Stem Cells Devel* 2014;23:380–92.
- [14] Klemm D, Kramer F, Moritz S, Lindstrom T, Ankerfors M, Gray D, et al. Nanocelluloses: a new family of nature-based materials. *Angew Chem Int Ed* 2011;50:5438–66.
- [15] Prestwich GD, Liu Y, Yu B, Shu XZ, Scott A. 3-D culture in synthetic extracellular matrices: new tissue models for drug toxicology and cancer drug discovery. *Adv Enzyme Regul* 2007;47:196–207.
- [16] Vanderhoof JL, Alcoutlabi M, Magda JJ, Prestwich GD. Rheological properties of cross-linked hyaluronan-gelatin hydrogels for tissue engineering. *Macromol Biosci* 2009;9:20–8.
- [17] Gripon P, Rumin S, Urban S, Le Seyec J, Glaize D, Canine I, et al. Infection of a human hepatoma cell line by hepatitis B virus. *Proc Natl Acad Sci* 2002;99:15655–60.
- [18] Cerec V, Glaize D, Garnier D, Morosan S, Turlin B, Drenou B, et al. Trans-differentiation of hepatocyte-like cells from the human hepatoma HepaRG cell line through bipotent progenitor. *Hepatology* 2007;45:957–67.

- [25] Ye J, Coulouris G, Zaretskaya I, Cutcutache I, Rozen S, Madden TL. Primer-BLAST: a tool to design target-specific primers for polymerase chain reaction. *BMC Bioinformatics* 2012;13.
- [26] Toivonen S, Ojala M, Hyysalo A, Ilmarinen T, Rajala K, Pekkanen-Mattila M, et al. Comparative analysis of targeted differentiation of human induced pluripotent stem cells (hiPSCs) and human embryonic stem cells reveals variability associated with incomplete transgene silencing in retrovirally derived hiPSC lines. *Stem Cells Transl Med* 2013;2:83–93.
- [27] Mikkola M, Olsson C, Palgi J, Ustinov J, Palomaki T, Horelli-Kuitunen N, et al. Distinct differentiation characteristics of individual human embryonic stem cell lines. *BMC Dev Biol* 2006;6:40.
- [28] Malinen MM, Palokangas H, Yliperttula M, Urtti A. Peptide nanofiber hydrogel induces formation of bile canaliculi structures in three-dimensional hepatic cell culture. *Tissue Engn Part A* 2012;18:2418–25.
- [29] Meisenheimer PL, Uyeda HT, Ma DP, Sobol M, McDougall MG, Corona C, et al. Proluciferin acetals as bioluminescent substrates for cytochrome P450 activity and probes for CYP3A inhibition. *Drug Metab Dispos* 2011;39:2403–10.
- [30] Aninat C, Piton A, Glaise D, Le Charpentier T, Langouet S, Morel F, et al. Expression of cytochromes P450, conjugating enzymes and nuclear receptors in human hepatoma HepaRG cells. *Drug Metab Dispos* 2006;34:75–83.
- [31] Chen YT, Sonnaert M, Roberts SJ, Luyten FP, Schrooten J. Validation of a pico green-based DNA quantification integrated in an RNA extraction method for two-dimensional and three-dimensional cell cultures. *Tissue Engn Part C* 2012;18:444–52.
- [32] Barth CA, Schwarz LR. Transcellular transport of fluorescein in hepatocyte monolayers: evidence for functional polarity of cells in culture. *Proc Natl Acad Sci* 1982;79:4985–7.
- [33] Bravo P, Bender V, Cassio D. Efficient in vitro vectorial transport of a fluorescently conjugated bile acid analogue by polarized hepatic hybrid WIF-B and WIF-B9 cells. *Hepatology* 1998;27:576–83.
- [34] Lai Y, Xing L, Poda GI, Hu Y. Structure-activity relationships for interaction with multidrug resistance protein 2 (ABCC2/MRP2): the role of torsion angle for a series of biphenyl-substituted heterocycles. *Drug Metab Dispos* 2007;35:937–45.
- [35] Godoy P, Hewitt NJ, Albrecht U, Andersen ME, Ansari N, Bhattacharya S, et al. Recent advances in 2D and 3D in vitro systems using primary hepatocytes, alternative hepatocyte sources and non-parenchymal liver cells and their use in investigating mechanisms of hepatotoxicity, cell signaling and ADME. *Arch Toxicol* 2013;87:1315–530.
- [36] Hart SN, Li Y, Nakamoto K, Subileau EA, Steen D, Zhong XB. A comparison of whole genome gene expression profiles of HepaRG cells and HepG2 cells to primary human hepatocytes and human liver tissues. *Drug Metab Dispos* 2010;38:988–94.
- [37] Gunness P, Mueller D, Shevchenko V, Heinzle E, Ingelman-Sundberg M, Noor F. 3D Organotypic cultures of human HepaRG cells: a tool for in vitro toxicity studies. *Toxicol Sci* 2013;133:67–78.
- [38] Vartiainen J, Pohler T, Sirola K, Pylkkanen L, Alenius H, Hokkinen J, et al. Health and environmental safety aspects of friction grinding and spray drying of microfibrillated cellulose. *Cellulose* 2011;18:775–86.
- [39] Ghosh K, Pan Z, Guan E, Ge S, Liu Y, Nakamura T, et al. Cell adaptation to a physiologically relevant ECM mimic with different viscoelastic properties. *Biomaterials* 2007;28:671–9.
- [40] Liu Y, Shu XZ, Gray SD, Prestwich GD. Disulfide-crosslinked hyaluronan-gelatin sponge: growth of fibrous tissue in vivo. *J Biomed Mater Res A* 2004;68:142–9.
- [41] Karpinen A, Saarinen T, Salmela J, Laukkanen A, Nuopponen M, Seppala J. Flocculation of microfibrillated cellulose in shear flow. *Cellulose* 2012;19:1807–19.
- [42] Paakko M, Ankerfors M, Kosonen H, Nykanen A, Ahola S, Osterberg M, et al. Enzymatic hydrolysis combined with mechanical shearing and high-pressure homogenization for nanoscale cellulose fibrils and strong gels. *Biomacromolecules* 2007;8:1934–41.
- [43] Lambert CB, Spire C, Claude N, Guillouzo A. Dose- and time-dependent effects of phenobarbital on gene expression profiling in human hepatoma HepaRG cells. *Toxicol Appl Pharmacol* 2009;234:345–60.
- [44] Le Vee M, Jigorel E, Glaise D, Gripon P, Guguen-Guillouzo C, Fardel O. Functional expression of sinusoidal and canalicular hepatic drug transporters in the differentiated human hepatoma HepaRG cell line. *Eur J Pharm Sci* 2006;28:109–17.
- [45] Wang EJ, Casciano CN, Clement RP, Johnson WW. Fluorescent substrates of sister-P-glycoprotein (BSEP) evaluated as markers of active transport and inhibition: evidence for contingent unequal binding sites. *Pharm Res* 2003;20:537–44.
- [46] Feller N, Broxterman HJ, Wahrer DCR, Pinedo HM. Atp-dependent efflux of calcein by the multidrug-resistance protein (MRP) – no inhibition by intracellular glutathione depletion. *FEBS Lett* 1995;368:385–8.
- [47] Litman T, Brangi M, Hudson E, Fetsch P, Abati A, Ross DD, et al. The multidrug-resistant phenotype associated with overexpression of the new ABC half-transporter, MXR (ABCG2). *J Cell Sci* 2000;113(Pt 11):2011–21.